# NEUTRONIC DESIGN OF IRRADIATION DEVICE FOR NEUTRON TRANSMUTATION DOPING IN HANARO

**Byung Jin Jun, Young Dong Song, Myong Seop Kim and Byung Chul Lee**
Korea Atomic Energy Research Institute
P.O. Box 105, Yuseong, Daejeon, 305-600, Korea
bjjun@kaeri.re.kr; mskim@kaeri.re.kr; bclee2@kaeri.re.kr

## ABSTRACT

HANARO has two vertical holes in the heavy water reflector region for neutron transmutation doping(NTD) - NTD1 and NTD2 of which diameters are 22 and 18cm respectively. We are developing an irradiation device for commercial NTD service using NTD2 hole. Uniform irradiation for the larger ingot by length as well as by diameter is the prime target of the irradiation device design. The neutron screen method is chosen for the uniform irradiation considering the situation of irradiation hole and throughput of irradiation service. In order to minimize generation of long-lived radwaste during experiment to search optimum configuration of the neutron screen, neutron absorber material such as stainless steel or nickel is avoided for the screen. The combination of water, Al and void is chosen instead, and the actual material of the screen is aluminum. VENTURE and MCNP are used for the prediction of flux distribution. The radial uniformity of irradiation is confirmed by calculation assuming rotation of the ingot during irradiation. The average flux is lowest at the center and highest at the periphery of the ingot, but the difference is less than 3%. Calculations show that the axial flux shape is almost the same if it is shifted properly depending on the control rod position. Therefore, we design the neutron screen with adjustable position with an ingot inside. The optimum neutron screen is searched for a fixed reactor condition so as to give the axial flux non-uniformity less than ±1.5%.

## 1. INTRODUCTION

HANARO has two vertical through holes in the heavy water reflector region for NTD as shown in Fig. 1 - NTD1 and NTD2 of which diameters are 22 and 18cm respectively. A feasibility study[1] confirmed that the two holes are very good for the NTD from the viewpoints of neutron quality and size. While fast neutron causing defects in the crystal and gamma heat increasing temperature in the ingot are sufficiently low, thermal neutron flux is high for not so long irradiation time. Both holes can be used for the irradiation of 6” ingot of which diameter is the largest in the current market of floating zone Si single crystal (FZ-Si). NTD1 can be used for irradiation of the larger diameter ingot which would be introduced to the market in the future. The good feature of NTD holes encouraged us to develop irradiation devices for the commercial NTD service.

Uniform irradiation for the larger ingot by length as well as by diameter is the prime target of the irradiation device design. A mean to achieve accurate fluence corresponding to the target resistivity such as the real time monitoring of the neutron flux should also be considered. For the first phase of the device development, we chose simultaneous irradiation of two pieces of 5” ingot with 30cm length at the NTD2 hole, considering the major demand in the current market. Expanded use of this

hole for the 6” ingot as the second phase in the near future and application of similar device concept to the NTD1 hole as the third phase are also considered at first phase work. We are developing the first phase device and this paper presents the work focusing on neutronic design.

## 2. DESIGN OF IRRADIATION DEVICE

### 2.1 NTD STRATEGY

A preliminary study showed that the thermal-to-fast flux ratio is large enough and the gamma heat is sufficiently low for the NTD. In the first phase, we intended to develop an NTD device using the NTD2 hole for 5" irradiation. When we have confidence on our technology, we will develop 6" irradiation device at the same hole in the second phase. This 6" irradiation device will accommodate 5" ingots as well. After then we will develop a device using the NTD1 hole for the irradiation of 6" or the larger one. The target length of an ingot is 60 cm for every case.

The flux screen method is the only option practically possible and would be the best in HANARO for high NTD capacity. Since the available space below the hole is not enough to move the ingot fully downward, traveling method as in BR2[2] or other reactors cannot be used. The axial flux profile is similar with cosine shape and the region of linear flux variation is not long enough. Therefore, turning over after a half irradiation technique of which is found in JRR-3M and JRR-3[3] is not proper. The axial flux distribution varies as the control rod position or core condition changes, but calculations confirmed that while the axial flux profile shifts or its magnitude changes at the NTD hole, their shapes are kept almost the same. It encouraged us to search a flux screen of fixed geometry with the capability of adjusting its axial position. Relatively strong neutron absorber compared to water such as stainless steel or nickel was avoided for the material of flux screen in the first phase. The combination of water, aluminum and void are chosen instead, in order to minimize the production of long half-lived radwaste during the trial and error stage to search an optimum geometry of flux screen by experiments. An effort has been also given to maximize the neutron flux in the ingot.

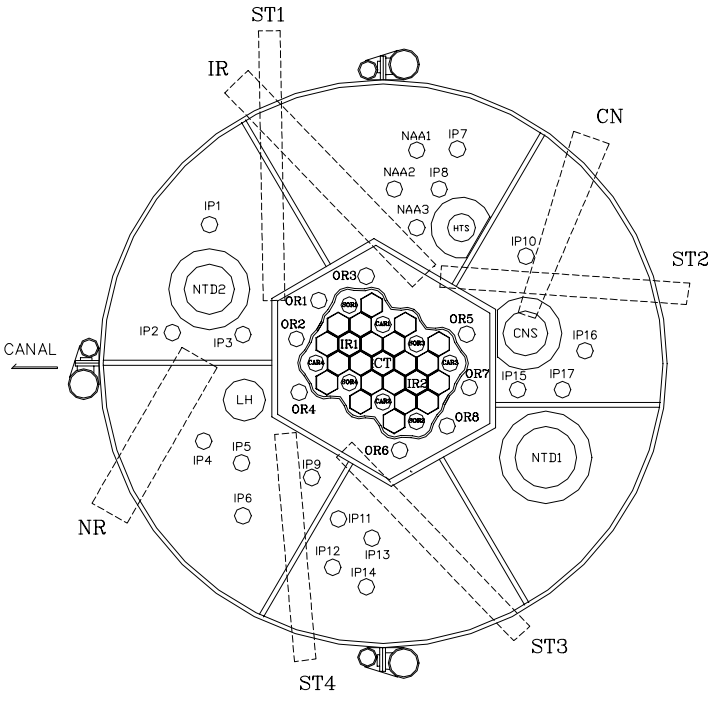


Figure 1. Location of NTD Holes in HANARO

One of the objectives of the first phase is confirming the accuracy and error trend in the prediction of flux distribution at the ingot with designed screen. In the second phase, stainless steel or nickel should be used for the screen because the gap between the inner wall of the NTD2 hole and the ingot surface becomes much thin

for 6" irradiation. The data obtained in the first phase are expected to help us avoid any trial and errors in the next phases.

Insertion of an ingot into the NTD hole replaces water by silicon, which increases neutron flux not only in the NTD hole but also nearby experimental holes and neutron detectors for reactor operation. If it is significant, a method should be searched to prevent the interference with other experiments or reactor operation. For this purpose, the effect of NTD to other places is calculated. The effect to core reactivity is almost negligible.

## 2.2 VERIFICATION OF CALCULATION

VENTURE[4] and MCNP[5] are used for the prediction of flux distribution. The geometry of the flux screen is rather complicated for the HANARO fuel management system (HANAFMS) [6] of WIMS[7] and VENTURE to deal with properly by the node homogenization technique. Therefore, MCNP has been used for the search of a proper flux screen. Since it does not have burnup capability yet, all fuels have been assumed as fresh. The effect of fuel burnup was obtained by the HANAFMS. It was also used for sensitivity calculations such as axial flux profile change depending on control rod position for simple geometry before the search.

The effect of fuel burnup to the flux distribution in the ingot was investigated by HANAFMS. The reliability of HANAFMS was checked first by comparing its result with that of MCNP for a fresh core. Although the general reliability of HANAFMS and MCNP had been confirmed many times through other experiments including the reactor commissioning tests, it was intended to reconfirm it for the specific case of NTD. The results of the fresh and burnt core calculated by HANAFMS were compared. Fig. 2 shows the model in the NTD2 hole for these calculations. A stack of aluminum disks simulates the silicon ingot. The air gap surrounding the Al is the space for the flux screen. An air chamber is provided below the Al. It will occupy the central region of the hole when the ingot is withdrawn.

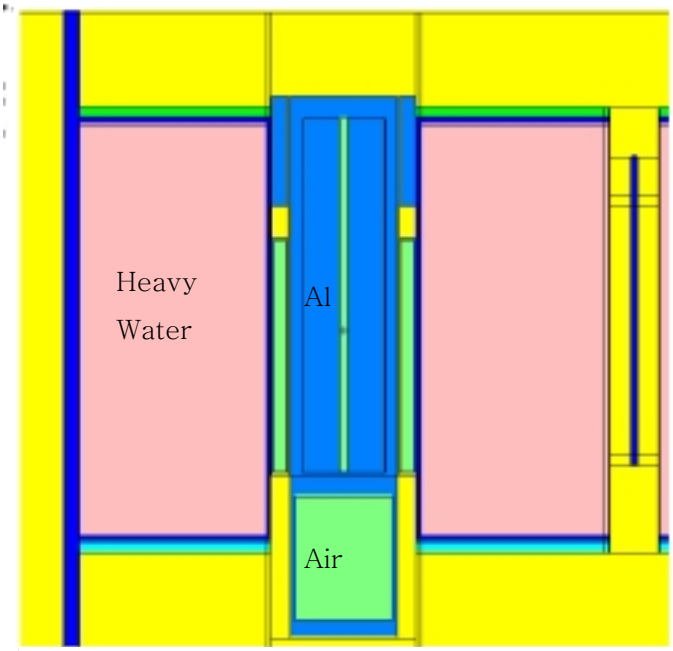


Figure 2. NTD2 Hole Model for Calculation

Fig. 3 compares the axial flux distribution in the aluminum region. For the fresh core, HANAFMS and MCNP give almost the same flux distribution. For the burnt core, HANAFMS shows about 20 % higher flux than the fresh core. It agrees very well with the average U-235 burnup in the core, which is roughly 20 %. In order to check the change of flux shape, each flux distribution is normalized to the maximum and results are depicted in Fig. 4. The location of ingot will be approximately from -35 to 25 cm. In this region, the burnt core shows slightly flatter distribution than the fresh core.

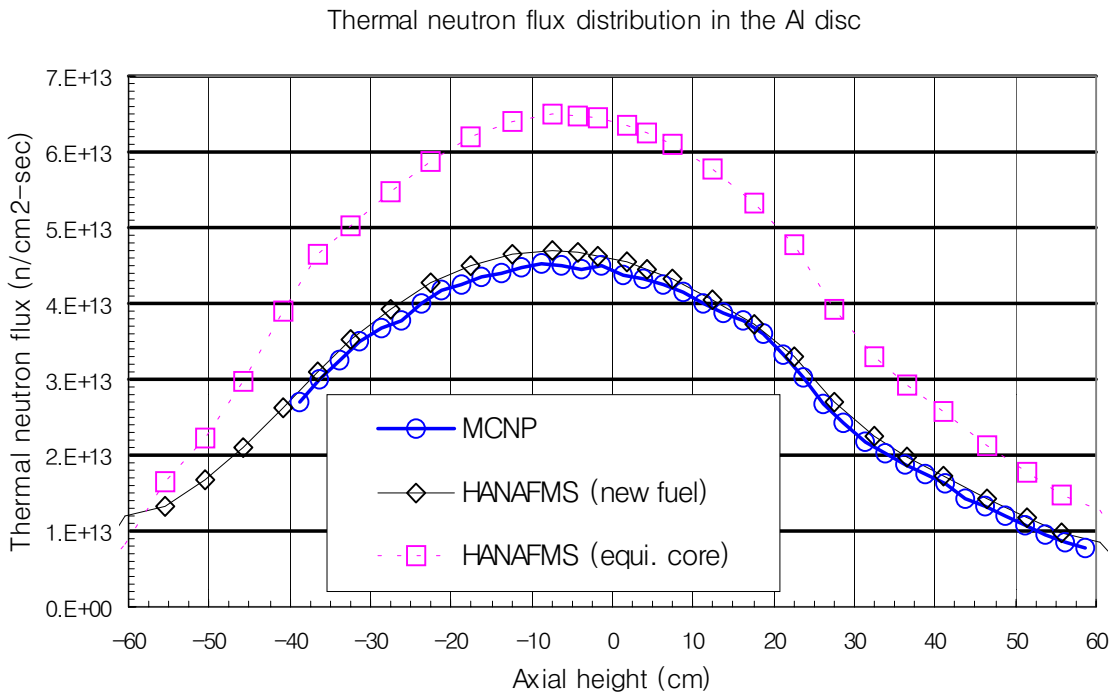


Figure 3. Axial Flux Distributions in Aluminum of Figure 2 at 24 MW

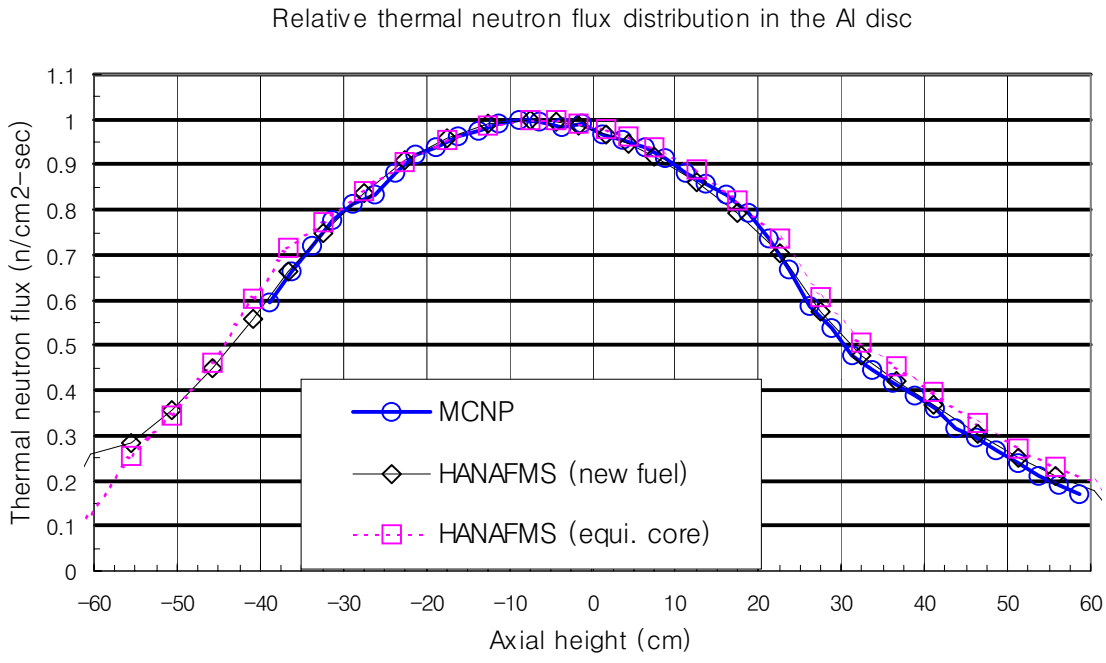


Figure 4. Relative Flux Distributions of Figure 3

Simulation experiments were carried out using aluminum, and flux distributions were measured. The measured data were compared with calculations to confirm the reliability of further calculations.

Au-wire activation method was used for the flux distributions measurement. Fig. 5 shows the irradiation device for these experiments. The aluminum can with thick wall contains Al blocks inside. Each block has a hole at the center. This experimental device is actually modeled as Fig. 2 for calculation but the axial positions of Al can and disks are adjusted in the calculation as in the actual experiment. For the axial flux distribution measurement, a long Au wire was installed along the central hole. Some parts of the wire were covered by Cd tubes to measure Cd ratio. Two wires were attached at the side and top surface of each Al disk to measure azimuthal flux distribution. The wire wounding the side surface forms a circle of Al disc radius and the top surface wire forms a half radius circle. The measured average reaction rate of Au at each circle was almost the same with that at the center. The difference was within the measuring uncertainty.

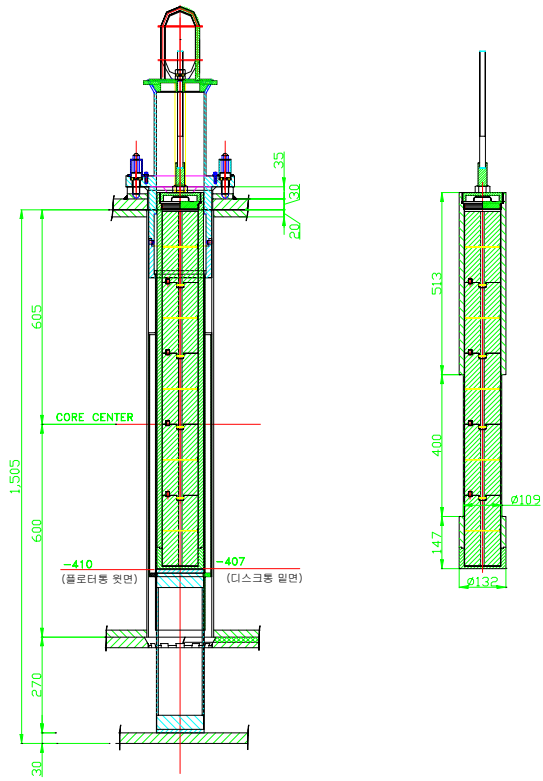


Figure 5. Irradiation Devices for the Flux Distribution Measurement

The first measurement was carried out with the original Al can depicted in the left hand side of Fig. 5. Fig. 6 compares the measured thermal neutron reaction rate with calculations. MCNP can give a total reaction rate but its statistics is bad because of a sharp and strong resonance of Au. Therefore, the thermal reaction rate is compared. HANAFMS gives thermal neutron flux but does not give thermal reaction rate. As a result of the MCNP calculation for this case, it is found that the distribution of the thermal neutron reaction rate is almost exactly the same as with the thermal neutron flux distribution. Therefore, the measured thermal neutron reaction rate can be compared with the thermal neutron flux. The reaction rate of non-thermal neutrons is subtracted from the total reaction rate to obtain a pure thermal neutron reaction rate.

The Cd ratio is measured at only 5 points. Deep wells in Fig. 6 are caused by Cd tube installations. All Cd ratios except at the top point showed small difference and the four values were fitted to obtain a position dependent Cd ratio. The Cd ratio at the top position was far larger than the other four points but the fitted values were used for whole length. It makes the measured thermal reaction rate at the upper region (35 - 60 cm in the figure) smaller than the actual values because of over-compensation of Cd ratio. It is the reason of a slightly higher trend of MCNP results than the measurement at the upper region. The HANAFMS shows much higher values than measurement in this region, which would come from the intrinsic limitation of diffusion theory for thick water zone surrounding the aluminum can. The figure indicates that the MCNP predicts the thermal neutron flux distribution in the ingot with good accuracy, and the effect of fuel burnup is very small.

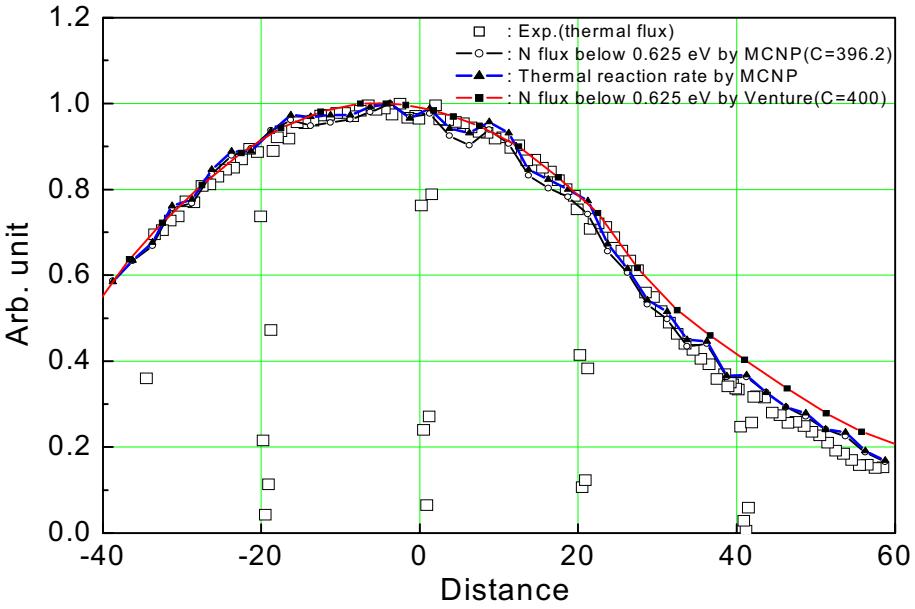


Figure 6. Comparison of First Measurement and Calculation

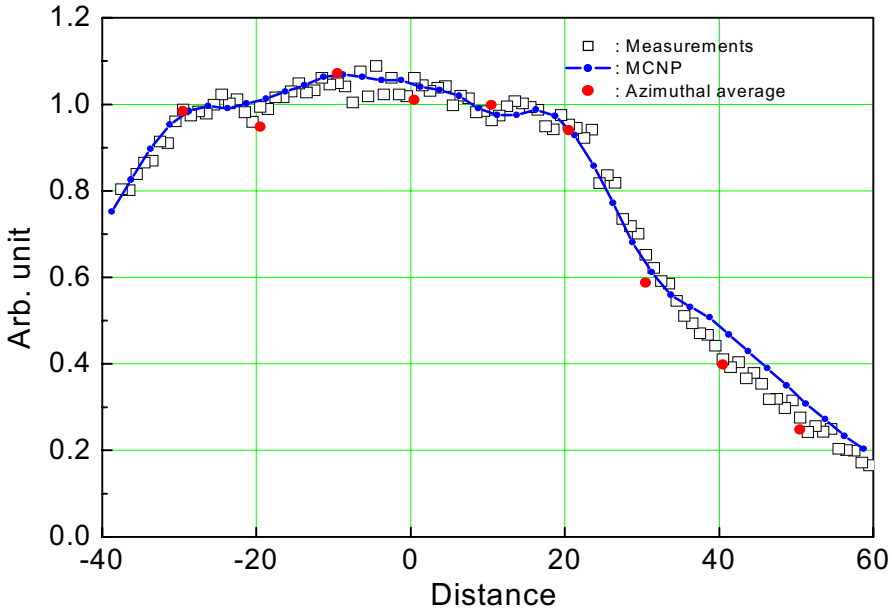


Figure 7. Comparison of Second Measurement and MCNP Calculation

The flux distribution was measured once again after the side surface of Al can is cut as the right hand side in Fig. 5. Since the cut region is replaced by water, the flux in this region is reduced as shown in Fig. 7. The Cd ratio was not measured at the second measurement and the values of the first measurement were used for compensation. The MCNP predicts well for this case, too.

## 2.3 FLUX SCREEN DESIGN AND ANALYSES

An optimum flux screen is searched for a fixed control rod position at 350 mm. Its cutaway view is depicted in Fig. 8. An aluminum sleeve is installed for the guidance of insertion and withdrawal of ingot can in the hole and for the installation of self-powered neutron detectors. It also guides the movement of bottom graphite can and vacant aluminum can from the bottom of the hole. The flux screen is a wall of the aluminum can containing the ingot. While the ingot can is not inserted into the irradiation hole, the graphite and vacant aluminum can be floated by buoyancy to occupy the central part of the hole. Since the buoyant force is slightly more than the mass gravity of the two cans, they are floated but an arm at the bottom of the vacant can prevents them from continued floating. The two cans keep the neutron flux high while the ingot can is withdrawn.

The axially flat neutron flux in the ingot region can be achieved by reducing the flux of high region but it also reduces the flux at the both ends of ingot where the flux is relatively low. Therefore, while the high flux region is surrounded by thick water to reduce the flux, graphite cans are placed below and above the ingot as a reflector. Fig. 9 is the predicted axial average flux distribution when this irradiation device is used. The estimated axial flux variation in the ingot region is within $\pm 1.5$ %. During the search, it has been intended to make a slightly convex distribution in the ingot region because the fuel burnup effect is expected to increase the flux at both end regions of the ingot slightly. The effect of fuel burnup would be very small as shown in Fig. 6 and 7, but 1 or 2 % increase at the ends of the ingot would much enhance the flux uniformity.

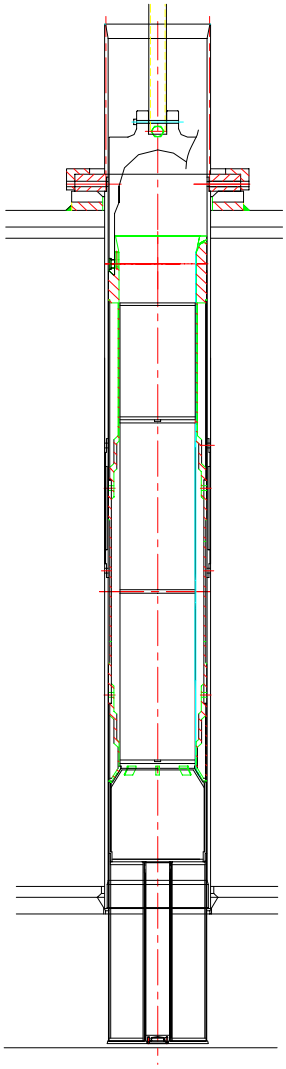

Figure 8. Cutaway View of NTD

In order to discover the flux change by the insertion of the ingot, the flux distributions in the irradiation hole are calculated for different conditions and they are compared in Fig. 10. The figure shows that the neutron flux with graphite and only the vacant cans is much higher than the case with the ingot can. Therefore, the flux in the hole decreases when the ingot can is inserted. In case the hole is simply filled with water, the flux is about a half of the case with ingot can. Therefore, if there is no floater in the hole, the flux increases by the insertion of the ingot can. This flux change affects other experimental holes nearby but not the inner holes closer to the core. The fluxes at IP1, IP2 and NR nose change in the same trend as Fig. 10 but by much less magnitude than the NTD hole. In case the floater exists, the maximum effect is about +5%. Without the floater, it is about –5%. IP3 and ST1 nose are also close to NTD2 but they are not affected because they are closer to the core than the NTD hole. The other holes are far enough to neglect the effect. Hence, the intention to reduce the flux change at the nearby holes is not

achieved. The achievement by using the floater is about 10 % higher flux at nearby holes when the ingot can is withdrawn.

The flux uniformity is checked when the control rods are at different positions. The optimum position of the flux screen is searched to get the most uniform flux distribution. Fig. 11 shows the relative flux distributions at different control absorber rod(CAR) positions. It indicates that the uniform flux distribution within ±2 % would be obtained by adjusting the position of the ingot can properly depending on the CAR position. The reference location of ingot can in Fig. 11 is –4.9 cm when the CAR is at 350 mm. Fig. 12 shows the searched optimum relation between the position of CARs and ingot can. It is found that the optimum position of the ingot can remains at almost the same location while the CAR position is within 250 to 350 mm. When that is above 350 mm, the relation is almost linear. The axially central position of the ingot is always below the core centerline because the flux shape is always tilted downward due to CARs.

## CONCLUSIONS

An optimum flux screen is searched for the NTD of 5" diameter and 60 cm length ingot at NTD2 hole of HANARO. Since the wall of the ingot can functions as the flux screen, its position can be adjusted to the optimum location depending on the CAR position. The axial uniformity within ±2 % is expected regardless of a control rod position, should position of the flux screen be properly adjusted. Slightly convex distribution of the neutron flux in the ingot region is intentionally chosen considering the fuel burnup effect, which would enhance the axial uniformity further. The actual flux distribution will be measured to confirm the accuracy of design prediction. It will help us avoiding trial and errors in the next phases: the development of 6" irradiation device for NTD2 hole in the second phase, and 6" and the larger ingot irradiation devices for NTD1 hole in the third phase.

## ACKNOWLEDGEMENTS

This paper is a part of the project funded by Ministry of Science and Technology of Korea.

## REFERENCES

1. B.J. Jun, et. al., “Analysis of NTD Method in HANARO”, *Proc. of 2002 KNS Autumn Meeting*, Daejeon, Korea, 26-27 October 2000 (written in Korean).
2. D.R. Cundy, et. al, “SIDONE - a new silicon irradiation facility in BR2”, *Proc. Intl. Conf. on Irradiation Tech.*, Saclay, France, 20-22 May 1992.
3. *Research reactor utilization hand book*, Research Reactor Department, Tokai Establishment, Japan Atomic Energy Research Institute (1999).
4. D.R. Vondy, et. al., “The BOLD VENTURE Computational System for Nuclear Reactor Core Analysis, Version III”, ORNL-5711, ORNL (1981).
5. J.F. Briesmeister, Ed., “MCNP-A General Monte Carlo N-Particle Transport Code, Version 4B”, LA-12625-M, LANL (1997).
6. H.R. Kim, et. al., “In-core Fuel Management Practice in HANARO”, *Nuclear Engineering and Design*, **Vol. 179**, pp. 281-286 (1998).
7. H.R. Kim, “WIMS-KAERI for the Extended KMRR Reactor Physics Calculation”, KAERI Internal Report, Korea Atomic Energy Research Institute (1987).

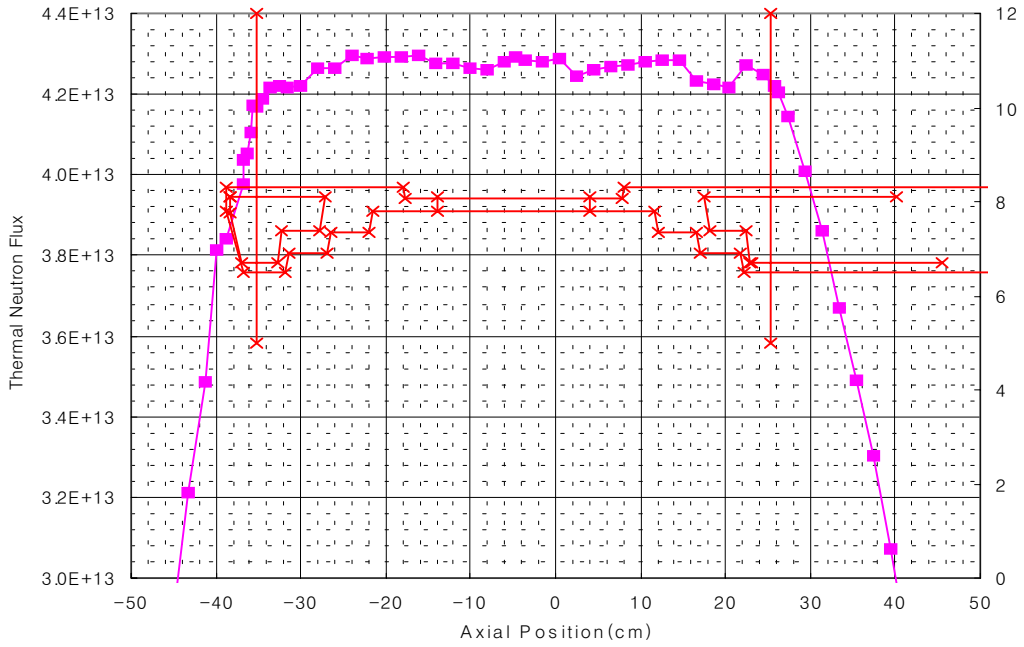


Figure 9. Predicted Flux Distribution with Optimized Flux Screen (CARs at 350mm, 24MW, Ingot Center at -4.9mm)

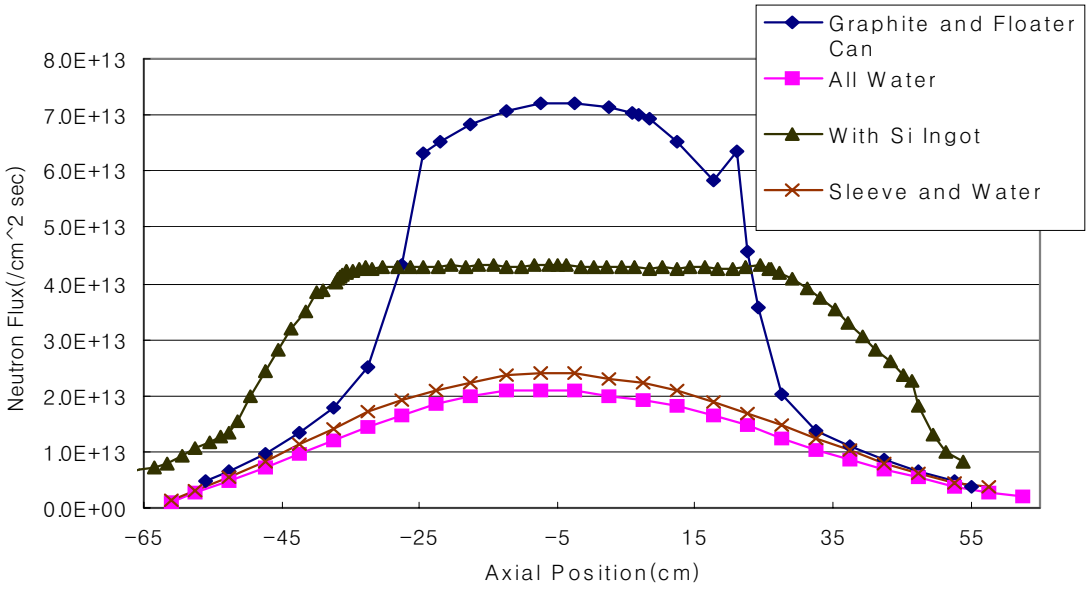


Figure 10. NTD2 Hole Neutron Flux (average within central 127.2 mm diameter circle) at Different Conditions (24MW)

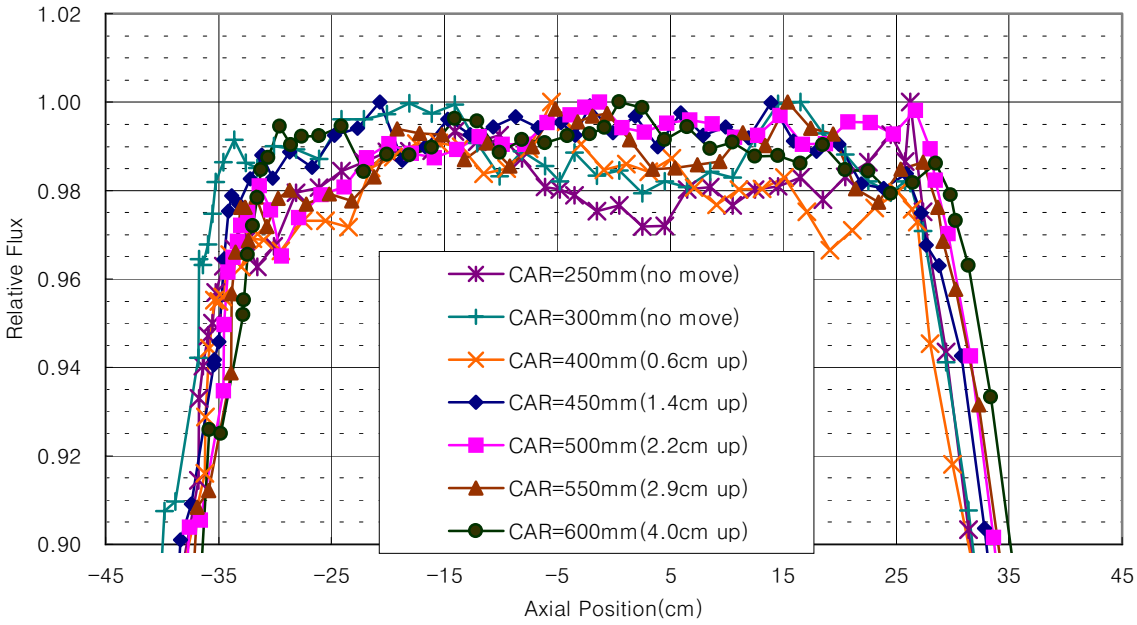


Figure 11. Relative Flux Distribution at Different Control Rod Positions

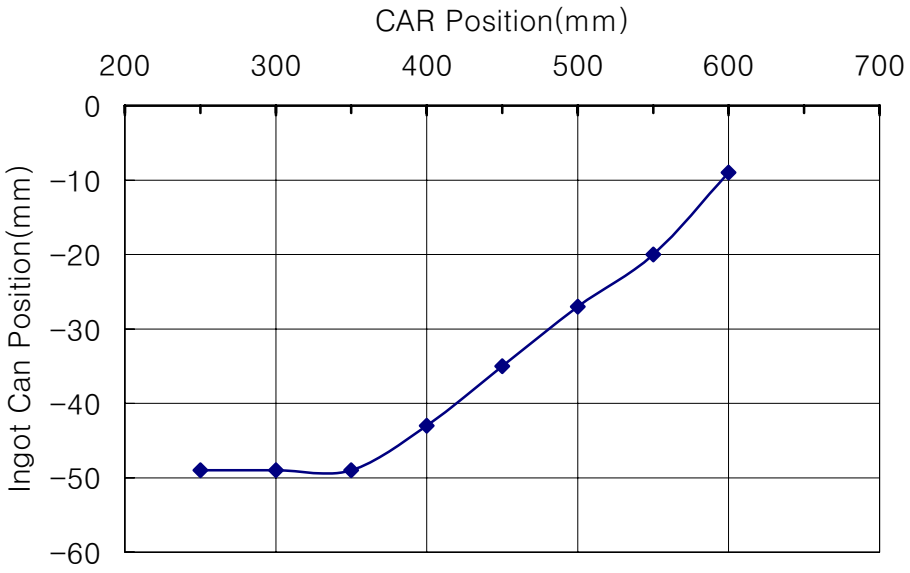


Figure 12. Optimum Position of Ingot Can Depending on CAR Position